| Journal of Coastal Research | 14 | 4 | 1325–1333 | Royal Palm Beach, Florida | Fall 1998 |
|---|---|---|---|---|---|

# Runup on Coastal Revetments Under the Influence of Onshore Wind

**Donald L. Ward†, Christopher G. Wibner‡ and Jun Zhang§**

† US Army Engineer Waterways Experiment Station CN-S
3909 Halls Ferry Road
Vicksburg, MS 39180, U.S.A.

‡ Aker Omega, Inc.
11757 Katy Freeway, Suite 1300
Houston, TX 77079, U.S.A.

§ Ocean Engineering Program
Department of Civil Engineering
Texas A&M University
Mail Stop 3136
College Station, TX 77843
U.S.A.

**ABSTRACT**

WARD, D.L.; WIBNER, C.G., and ZHANG, J., 1998. Runup on coastal revetments under the influence of onshore wind. *Journal of Coastal Research,* 14(4), 1325–1333. Royal Palm Beach (Florida), ISSN 0749-0208.

Height of maximum wave runup on coastal structures is typically calculated directly or indirectly from small-scale physical model tests. These tests are conducted in the absence of wind, although strong onshore winds are typically associated with design storms. To study the effects of onshore winds on runup elevations, a series of physical model tests has been conducted in a combined wind/wave flume at Texas A&M University. Low wind speeds were seen to have little effect on runup elevations, but higher wind speeds significantly increased runup elevations on both smooth and rough slopes. Wind effects were greater on steep slopes than on shallow slopes, and greater on smooth slopes than on rough slopes. Various mechanisms by which wind may affect runup are discussed.

**ADDITIONAL INDEX WORDS:** *Coastal engineering, coastal structures, physical model, none.*

## INTRODUCTION

The ability to accurately predict the vertical distance a wave will run up a revetment or other coastal structure is essential to determining design crest elevation for the structure. Traditionally, runup distances have been calculated from empirical equations determined from series of small-scale physical model tests (*e.g.,* WEGGEL, 1979; AHRENS and MARTIN, 1985; AHRENS and HEIMBAUGH, 1988, DE WAAL and VAN DER MEER, 1992, WARD, 1992; YAMAMOTO and HORIKAWA, 1992; VAN DER MEER and JANSSEN, 1994), from numerical models calibrated with small-scale physical model studies (*e.g.,* KOBAYASHI and WURJANTO, 1989; WURJANTO and KOBAYASHI, 1991; VAN DER MEER *et al.,* 1992; KOBAYASHI and POFF, 1994), or determined directly from physical model tests. In none of these cases is provision made for the influence of an onshore wind. Unfortunately, design storm conditions typically assume very strong onshore winds that may significantly affect runup elevations.

Because of the importance of accurate estimates of runup heights, the Coastal and Hydraulics Laboratory of the US Army Engineer Waterways Experiment Station has initiated a joint research project with Texas A&M University (TAMU) to investigate effects of onshore winds on runup of coastal revetments. Using a wave flume with wind-generating capabilities at TAMU, a series of tests was conducted on model revetments using a range of structure slopes, incident wave conditions, and wind speeds. Runup elevations were measured, along with changes in incident wave spectra due to the influence of wind.

The presence of wind may affect wave runup on a coastal structure in the following ways:

(a) wind-induced setup
(b) increased wave energy
(c) wind effects "pushing" a runup bore up the structure slope
(d) changes in wave kinematics due to wind effects on wave shape or wave breaking.

In a typical physical model study of a design storm on an existing or proposed coastal structure, a still water level and incident wave conditions are provided. The design still water level should include tidal conditions, storm surge, and wind-induced setup. Each of these may be calculated separately and examined using probabilistic methods to arrive at the prototype design water level. The water level in the physical model study may then be adjusted such that water depth at the structure toe in the presence of wind-induced setup will properly scale to the design water level in the prototype. Wind-induced setup in the study reported herein therefore is subtracted from measured runup elevations to yield runup above the still water level that is obtained in the presence of onshore winds.

Many studies have been conducted on the growth of waves in the presence of wind (a review of different approaches to wind-wave prediction may be found in SOBEY 1986), and this topic will not be considered here. It is recognized that a fully-developed sea does not experience wave growth in deep water under constant wind conditions, yet there is considerable wind-induced wave growth in the model flume. For the study reported herein, it is assumed that design wave conditions

*97018 received 15 February 1997; accepted in revision 25 October 1997.*

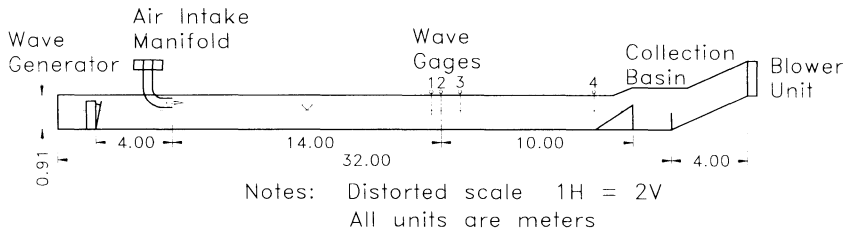


Figure 1. Wind/wave flume at Texas A&M University.

are known at the prototype structure, and it is a goal of the physical model study to reproduce prototype conditions, at a suitable scale, at the model structure. Wind-induced wave energy growth therefore may be separated from the analysis.

The study reported herein attempts investigated the increase in wave runup due to wind forces acting on the runup bore and due to changes in wave kinematics resulting from wind-induced wave breaking or changes in wave shape.

## TEST FACILITY

The two-dimensional wind/wave flume at TAMU is a glass-walled flume 36.0-m-long by 0.6-m-wide and 0.9-m-deep (Figure 1). Wave generation was by a pair of Seasim Ltd. (presently Commercial Hydraulics) RSW 30-60 dry-back hinged-flap wavemakers. Power was provided by a low inertia D.C. servo motor with sensors for position and velocity monitoring along with an adjustable compensation unit to balance the hydrostatic pressure. Wave generation was controlled by a standard IBM personal computer interfaced to the wavemaker through an analog output card using software developed at TAMU.

Wind generation was provided by an exhaust blower connected to the end of the flume away from the wavemakers. Air was pulled into the flume through a vertically-adjustable intake manifold equipped with horizontal vanes to help provide a uniform flow field in the flume.

Runup tests were conducted with plywood test structures with slopes of 1:1.5 (V : H), 1:3, and 1:5. Tests were conducted on both smooth and rough slopes, where the rough slopes were covered with a filter layer and two-layer-thick riprap armor layer designed in accordance with Engineering Manual EM 1110-2-1614 (U.S. ARMY ENGINEER COASTAL ENGINEERING RESEARCH CENTER, 1995).

Table 1. *Mechanical wave test conditions for runup tests. Each wave period/wave height combination was tested with wind speeds of 0 m/sec, 6.5 m/sec, 12.0 m/sec, and 16.0 m/sec.*

| Wave Period (sec) | Wave Height (m) | Wave Steepness (ka) |
|---|---|---|
| 1.0 | 0.050 | 0.104 |
| | 0.070 | 0.146 |
| | 0.100 | 0.208 |
| 1.75 | 0.032 | 0.029 |
| | 0.054 | 0.049 |
| 2.5 | 0.022 | 0.013 |
| | 0.038 | 0.023 |

Data acquisition was through a high-speed analog I/O board installed in a personal computer with automatic triggering of the control unit through a programmable interval timer linked to the wave generation personal computer. Data inputs included twin-rod resistance-type wave gauges, resistance-type and capacitance-type runup gauges on the test structures, and a three-cup anemometer for measuring wind speeds. In addition, visual observations of runup elevations were recorded and wind speed was measured by a pitot-static tube connected to an oil-filled manometer with wind speeds being visually observed.

## TEST PROCEDURE AND RESULTS

### Determination of Incident Wave Conditions

All tests were conducted with monochromatic waves produced in short bursts such that wave generation would cease before waves reflecting off the test structures could reach the wave board and contaminate the incident wave train. Three wave periods were tested, with two or three wave heights for each wave period for a total of seven wave period/wave height combinations (Table 1). For each wave period/wave height combination, four wind speeds (including no-wind condition) were tested for a total of 28 different test conditions. Selection of wave heights was limited by the capabilities of the wavemaker; wind speeds corresponded to 50%, 75%, and 100% of blower capacity, as well as the no-wind condition. All tests were conducted with a no-wind still water level of 0.5 m.

A 1:5 plywood slope was placed in the flume and covered with several layers of rubber matting ("horse hair") to a thickness of approximately 30 cm near the toe and 23 cm near the crest to absorb wave energy and minimize reflection. A wave gauge placed near the structure toe (26 m from the wavemaker) recorded the incident wave train. The method of GODA and SUZUKI (1976) was used to examine the recorded signals from a set of wave gauges centered 24 m in front of the wavemaker to separate incident and reflected wave trains and confirm that reflection was minimal. Each of the 28 test conditions was run with the wave-absorbing slope to establish incident wave conditions. Results are given in Table 2; energy spectra for each of the seven wave period/wave height combinations are illustrated in Figures 2 through 8.

To minimize water losses from splash and spray, and to avoid significant sloshing in the flume caused by wind forcing, wind was blown in the flume for only two minutes to establish the wind-generated wave field before beginning me-

Table 2. *Incident wave parameters.*

| Case | Wind Velocity (m/sec) | Period (mech.) (sec) | Period (wind) (sec) | Energy (mech.) ($cm^2$) | Energy (wind) ($cm^2$) | $H_S$ (cm) | Reflection Coeff. |
|---|---|---|---|---|---|---|---|
| 1a | 0.0 | 1.0 | 0.00 | 6.803 | 0.000 | 4.89 | 0.061 |
| 1b | 6.5 | 1.0 | 0.00 | 7.740 | 0.000 | 6.66 | 0.084 |
| 1c | 12.0 | 1.0 | 0.00 | 12.319 | 0.000 | 9.99 | 0.108 |
| 1d | 16.0 | 1.0 | 0.00 | 19.373 | 0.000 | 15.82 | 0.078 |
| 2a | 0.0 | 1.0 | 0.00 | 9.353 | 0.000 | 6.77 | 0.056 |
| 2b | 6.5 | 1.0 | 0.00 | 10.503 | 0.000 | 8.35 | 0.077 |
| 2c | 12.0 | 1.0 | 0.00 | 16.086 | 0.000 | 13.04 | 0.09 |
| 2d | 16.0 | 1.0 | 0.00 | 32.649 | 0.000 | 18.73 | 0.068 |
| 3a | 0.0 | 1.0 | 0.00 | 11.321 | 0.000 | 10.00 | 0.042 |
| 3b | 6.5 | 1.0 | 0.00 | 12.702 | 0.000 | 11.59 | 0.065 |
| 3c | 12.0 | 1.0 | 0.00 | 29.396 | 0.000 | 17.64 | 0.080 |
| 3d | 16.0 | 1.0 | 0.00 | 32.083 | 0.000 | 19.57 | 0.051 |
| 4a | 0.0 | 1.75 | 0.00 | 1.062 | 0.000 | 2.96 | 0.219 |
| 4b | 6.5 | 1.75 | 0.55 | 1.208 | 1.015 | 4.85 | 0.225 |
| 4c | 12.0 | 1.75 | 0.64 | 1.649 | 3.449 | 7.38 | 0.242 |
| 4d | 16.0 | 1.75 | 0.71 | 2.679 | 5.827 | 9.80 | 0.275 |
| 5a | 0.0 | 1.75 | 0.00 | 3.213 | 0.000 | 5.26 | 0.222 |
| 5b | 6.5 | 1.75 | 0.59 | 3.531 | 0.855 | 7.29 | 0.224 |
| 5c | 12.0 | 1.75 | 0.71 | 4.409 | 3.388 | 9.00 | 0.229 |
| 5d | 16.0 | 1.75 | 0.90 | 7.693 | 3.439 | 11.68 | 0.257 |
| 6a | 0.0 | 2.5 | 0.00 | 0.664 | 0.000 | 2.33 | 0.382 |
| 6b | 6.5 | 2.5 | 0.55 | 0.719 | 0.760 | 4.44 | 0.381 |
| 6c | 12.0 | 2.5 | 0.62 | 0.890 | 3.206 | 6.94 | 0.397 |
| 6d | 16.0 | 2.5 | 0.69 | 1.120 | 5.536 | 9.45 | 0.412 |
| 7a | 0.0 | 2.5 | 0.62 | 1.807 | 0.000 | 3.85 | 0.386 |
| 7b | 6.5 | 2.5 | 0.52 | 1.872 | 0.563 | 4.71 | 0.388 |
| 7c | 12.0 | 2.5 | 0.66 | 2.275 | 2.612 | 7.31 | 0.391 |
| 7d | 16.0 | 2.5 | 0.78 | 2.608 | 5.507 | 9.47 | 0.397 |
| 8a | 0.0 | 1.0 | 0.00 | 0.366 | 0.000 | 1.71 | 0.074 |
| 8b | 6.5 | 1.0 | 0.00 | 0.530 | 0.000 | 3.99 | 0.228 |
| 8c | 12.5 | 1.0 | 0.00 | 2.243 | 0.000 | 7.63 | 0.245 |
| 8d | 16.0 | 1.0 | 0.00 | 8.309 | 0.000 | 10.95 | 0.221 |
| 9a | 0.0 | 1.0 | 0.00 | 0.941 | 0.000 | 2.77 | 0.058 |
| 9b | 6.5 | 1.0 | 0.00 | 0.122 | 0.000 | 4.87 | 0.132 |
| 9c | 12.0 | 1.0 | 0.00 | 3.737 | 0.000 | 8.87 | 0.205 |
| 9d | 16.0 | 1.0 | 0.00 | 12.537 | 0.000 | 12.46 | 0.156 |
| 10a | 0.0 | 1.0 | 0.00 | 1.843 | 0.000 | 3.82 | 0.060 |
| 10b | 6.5 | 1.0 | 0.00 | 2.322 | 0.000 | 5.99 | 0.095 |
| 10c | 12.0 | 1.0 | 0.00 | 5.506 | 0.000 | 8.75 | 0.202 |
| 10d | 16.0 | 1.0 | 0.00 | 15.199 | 0.000 | 13.45 | 0.126 |
| 11a | 0.0 | 1.0 | 0.00 | 3.947 | 0.000 | 5.68 | 0.075 |
| 11b | 6.5 | 1.0 | 0.00 | 4.654 | 0.000 | 7.33 | 0.089 |
| 11c | 12.0 | 1.0 | 0.00 | 12.084 | 0.000 | 11.86 | 0.133 |
| 12a | 0.0 | 1.0 | 0.00 | 7.057 | 0.000 | 7.64 | 0.085 |
| 12b | 6.5 | 1.0 | 0.00 | 8.367 | 0.000 | 9.25 | 0.080 |
| 12c | 12.0 | 1.0 | 0.00 | 16.662 | 0.000 | 13.83 | 0.098 |
| 13a | 0.0 | 1.0 | 0.00 | 8.776 | 0.000 | 8.51 | 0.085 |
| 13b | 6.5 | 1.0 | 0.00 | 10.195 | 0.000 | 10.20 | 0.083 |
| 13c | 12.0 | 1.0 | 0.00 | 22.425 | 0.000 | 16.23 | 0.099 |

chanical wave generation. Because of the short time period prior to starting the wavemaker, it was necessary to examine the wind wave energy growth rate in the flume. For each of the 3 wind velocities used in this study, the wave spectrum was recorded by a wave gauge located 22 m in front of the wind input manifold (near the toe of the wave-absorbing slope and 26 m in front of the wave generator) for time durations of 2, 10, 20, and 30 minutes. The resulting changes in wave energy are given in Table 3 and the wave energy growth is illustrated for the highest wind speed in Figure 9. The increase in wave energy from 2 to 30 minutes proved to be insignificant, probably due to saturation of the wind-wave

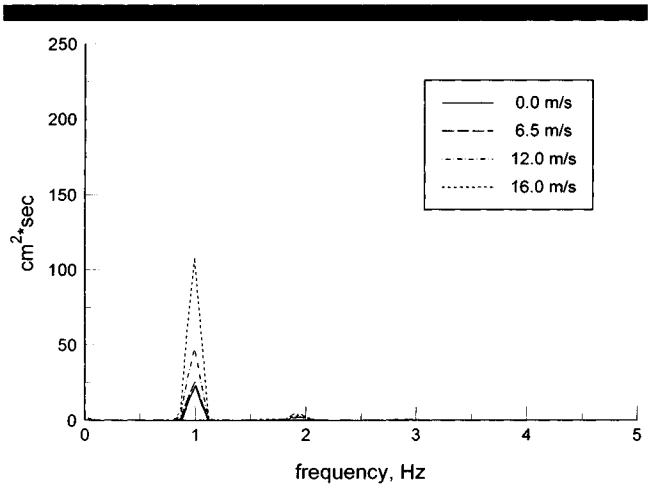


Figure 2. Energy spectra for 1-sec, 5.0-cm mechanical wave.

field resulting from the limited fetch length available in the flume. Therefore, two minutes was considered sufficient to establish the wind-generated wave field, and wind-wave energy was considered constant over the duration of each experimental test run.

During tests of wind-wave energy growth and tests to establish incident wave conditions for the combined wavemaker/wind generator tests, the amount of wind-induced setup at the revetment was measured. It was found that the wind-induced setup remained constant for each wind velocity, virtually independent of incident wave conditions or revetment slope. Observed wind-induced setup elevations are given in Table 4 for each of the wind speeds tested.

The addition of wind energy to the generated wave train clearly adds energy to the wave spectrum. Examination of Figures 5 through 8 for the wave spectra with mechanically-generated wave periods of 1.75 and 2.5 sec shows the majority of the energy increase due to wind in a second peak caused by wind-generated waves at a frequency of about 2 Hz. This

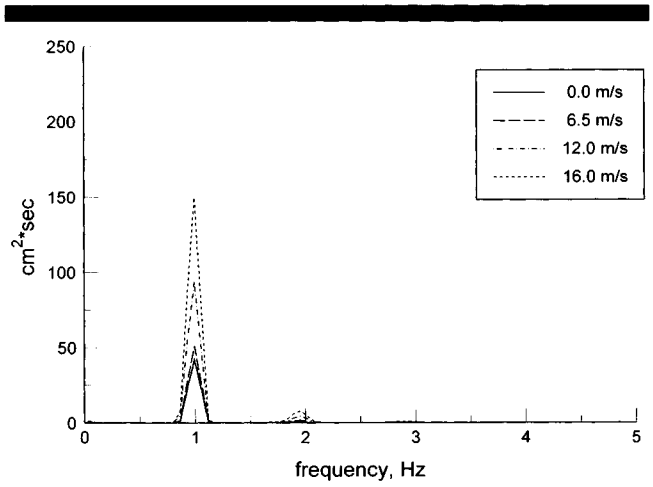


Figure 3. Energy spectra for 1-sec, 7.0-cm mechanical wave.

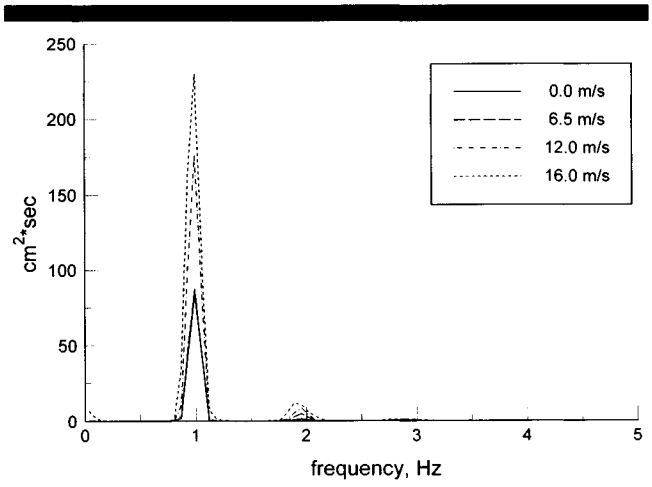


Figure 4. Energy spectra for 1-sec, 10.0-cm mechanical wave.

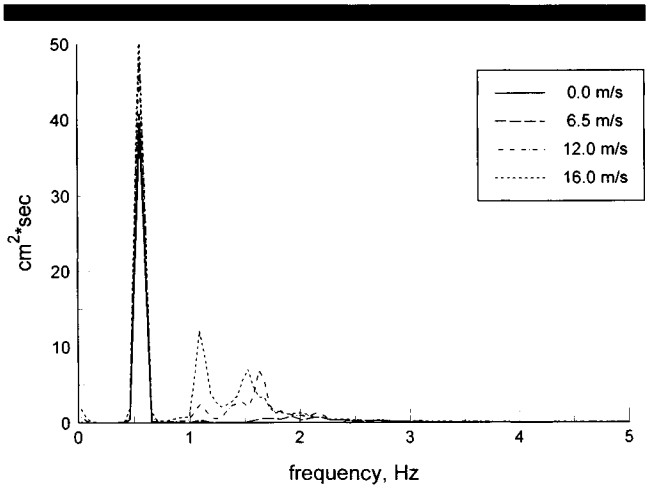


Figure 6. Energy spectra for 1.75-sec, 5.4-cm mechanical wave.

second peak is missing in Figures 2 through 4 for wave spectra with mechanically-generated wave periods of 1.0 sec, where the additional energy is shown as an increase in the single peak of the mechanically-generated wave. The primary reason the spectra of the one-second waves remain as a single peak was that as the wind-wave field developed during the first several meters of fetch, the wind-wave field was characterized by a high-frequency, short wave length wave field. As the steep one-second mechanically-generated waves propagated down the wind-wave flume, high frequency wind waves were blocked at the forward face of the steep mechanical waves and the wind waves were not allowed to form. This phenomenon of capillary/gravity wave blockage was described by ZHANG (1995), SHYU and PHILLIPS (1990) and PHILLIPS (1984). Phillips noted that while this phenomenon is not of great significance in the field, it can significantly affect the wave spectrum in laboratory wind-wave flumes with short fetches.

Modulation of the air pressure field also may have contributed to growth of the mechanically-generated one-second waves. Because the crests of the large mechanically-generated waves were closer to the top of the flume than were the troughs, airflow was constricted by reduction in cross-sectional area above the crests, resulting in higher local wind velocities at the crests. The opposite, of course, was true at the troughs. This modulation of wind velocities resulted in modulation of the air pressure field according to the Bernoulli equation. Modulated air pressures were in phase with mechanically-generated waves and led to the growth of mechanically-generated waves. Modulation of air pressure was not as significant for longer wave lengths because smaller wave heights were generated due to limitations of the wave generator.

## Runup Tests

For runup tests, the wave-absorbing slope was removed and test slopes of 1:1.5, 1:3, and 1:5 were installed. Each slope was tested both as a smooth slope and as a typical riprap

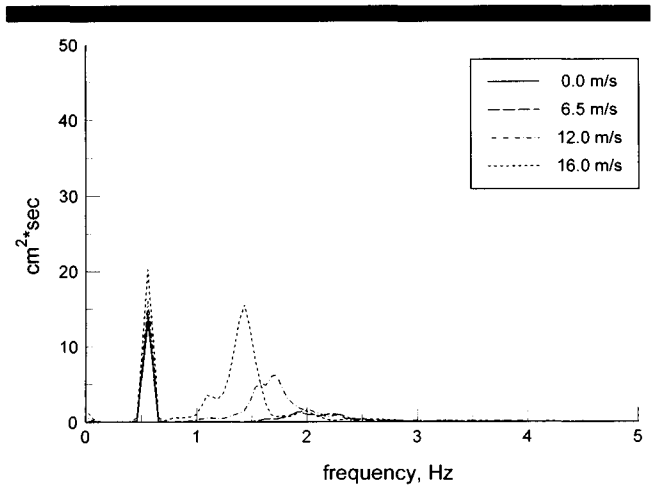


Figure 5. Energy spectra for 1.75-sec, 3.2-cm mechanical wave.

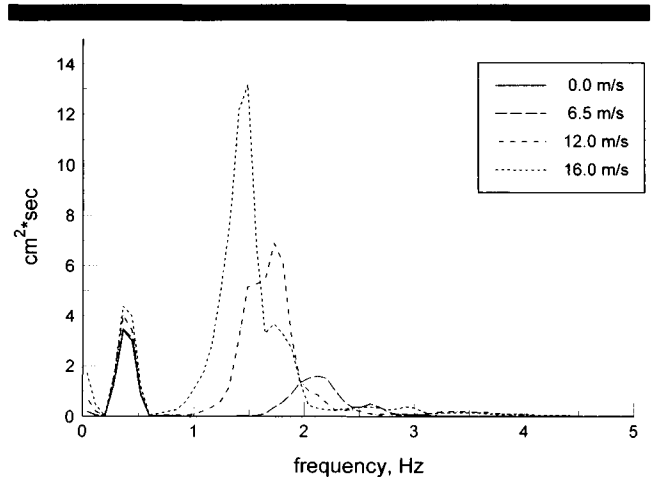


Figure 7. Energy spectra for 2.5-sec, 2.2-cm mechanical wave.

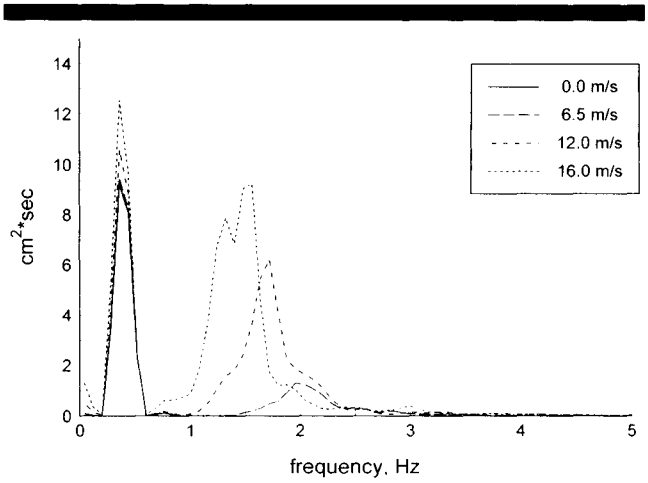


Figure 8. Energy spectra for 2.5-sec, 3.8-cm mechanical wave.

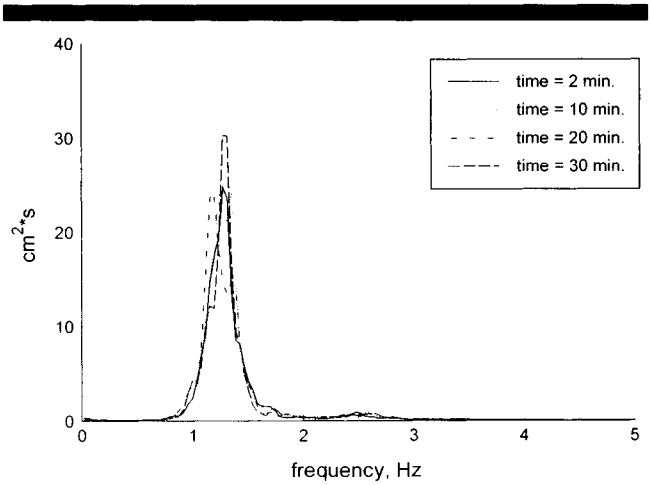


Figure 9. Wind wave energy spectrum growth for a wind velocity of 16 m/sec.

revetment at each of the 28 combinations of wave period/wave height/wind speed.

As seen in Figures 2 through 4, the addition of wind to a mechanically-generated wave period of 1 sec remained as a single-peaked spectrum. For these single-peaked cases, it is possible to determine wind effects on runup by mechanically reproducing the combined wind/wave spectra. That is, the stroke of the wave generator can be increased to produce a similar spectrum to that obtained by a lesser stroke under the influence of wind. Figures 10 through 15 plot runup elevations for tests with 1-sec wave periods including purely mechanically-generated waves and mechanically-generated waves under the influence of wind. The wind effects are clearly evident: for waves of similar wave height, runup is considerably greater when the wave height is obtained by a small mechanically-generated wave plus influence of a strong wind than when the wave height is purely mechanically driven (in the absence of wind).

It should be noted that runup illustrated in Figures 10 through 15, and in subsequent figures of runup, is that portion of the measured runup above the wind-induced setup. Wind-induced setup shown in Table 4 was subtracted from the measured runup elevations to yield an "equivalent runup," $R_{eq}$, for runup above the wind-induced still water level. The abscissa in these figures is the significant wave height, $H_s$ (average of one-third highest waves) determined with a zero down-crossing method. "Trend lines" have been added where appropriate for clarity.

In Figures 10 through 15, it is seen that effects of a 6.5 m/sec wind speed are negligible. The 12 m/sec wind speed produces a significant effect on the 1:1.5 rough slope and both 1:1.5 and 1:3 smooth slopes, but has negligible effect on flatter slopes. Only the 16 m/sec wind speed has a pronounced effect on runup on each of the three slopes tested.

Runup under the influence of the 12 m/sec wind and 16 m/sec wind is seen to increase linearly with incident wave height in Figures 10 through 15, then runup tapers off or even decreases with increasing incident wave height. This is due to wave breaking under the influence of wind prior to the wave reaching the test structure.

Table 3. *Wind-wave energy growth.*

| Wind Velocity (m/sec) | Time Duration (min) | Wind-Wave Energy ($cm^2$) | Peak Period (sec) |
|---|---|---|---|
| 6.5 | 2 | 4.262 | 0.534 |
| | 10 | 4.602 | 0.523 |
| | 20 | 4.444 | 0.523 |
| | 30 | 4.389 | 0.546 |
| 12.0 | 2 | 8.451 | 0.657 |
| | 10 | 7.711 | 0.711 |
| | 20 | 8.018 | 0.640 |
| | 30 | 8.276 | 0.656 |
| 16.0 | 2 | 11.064 | 0.775 |
| | 10 | 11.256 | 0.731 |
| | 20 | 11.309 | 0.825 |
| | 30 | 11.243 | 0.753 |

## Dual-Peaked Spectra

The addition of wind to mechanically-generated waves of periods 1.75 sec and 2.5 sec resulted in a second peak in the incident spectra due to wind generated waves (Figures 5 through 8). To examine the influence of wind on dual-peaked spectra, it is possible to mechanically reproduce a dual-peaked wind/wave spectrum and compare runup from the mechanically-generated spectrum and the wind/wave spectrum. In this study, the dual-peaked spectrum was reproduced mechanically by first generating the short wave portion of the spectrum (the high-frequency peak), then gener-

Table 4. *Wind-induced setup elevations.*

| Wind Velocity (m/sec) | Wind Induced Setup (cm) |
|---|---|
| 6.5 | 1.0 |
| 12.0 | 3.0 |
| 16.0 | 5.0 |

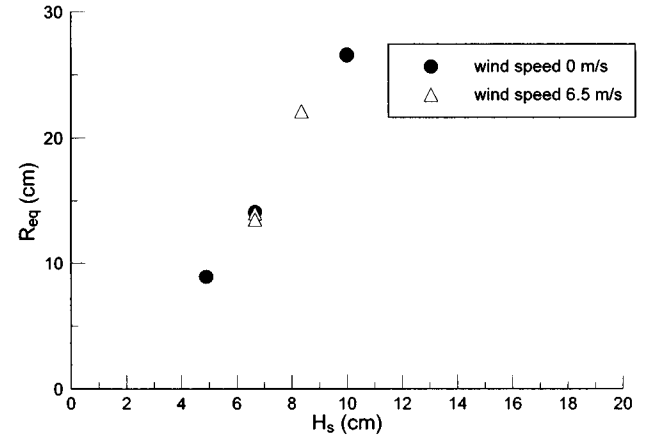


Figure 10. Equivalent runup comparison for 1-sec mechanical waves on a smooth 1:1.5 slope.

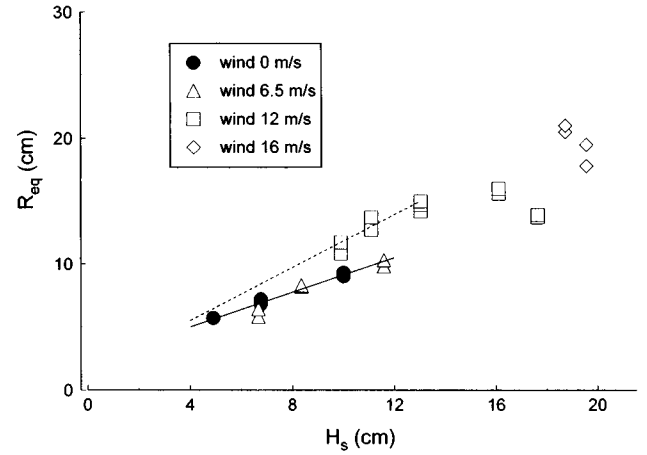


Figure 12. Equivalent runup comparison for 1-sec mechanical waves on a smooth 1:5 slope.

ating the long wave portion of the spectrum. Because the longer waves travel faster than the shorter waves, the longer waves will overtake the shorter waves to reproduce the dual-peaked spectrum near the test structure. Combined wind/wave dual-peaked spectra would change as they progressed down the flume; the goal of the mechanically-reproduced dual-peaked spectra was to match the wind/wave spectra recorded at the toe of the revetment. Trial-and-error was used to determine the wavemaker stroke necessary to reproduce the high-frequency peak of the dual-peaked spectrum. Monochromatic wave trains were used for both long and short waves in the mechanically-produced spectrum.

The wave maker used in this study was not able to reproduce the second peak in the spectra at 2 Hz, but was able to make a peak at about 1.6 Hz. As seen in Figure 16, the mechanically reproduced dual-peaked spectrum is very close to the wind/wave spectrum.

Due to limitations of the wavemaker, only some of the dual-peaked wind/wave spectra could be reproduced mechanically. Figure 17 plots runup on a smooth 1:3 slope for a (single-peak) mechanically-produced wave, the same mechanically-produced wave with wind effects adding a second peak to the wave energy spectrum, and the same mechanically-produced wave with a second set of mechanically-produced waves creating the second peak in the wave energy spectrum. It is again seen that runup is significantly higher in the presence of wind than from a similar spectrum produced mechanically.

Another method of estimating runup with a dual-peaked spectrum is to base the runup on an energy-based wave height and an "equivalent" wave period. Energy-based zeroth-moment wave heights may be readily obtained from dual-peaked spectra in the same manner as from single-peaked spectra, that is,

$$H_{m0} = 4^*\sqrt{m_0} \quad (1)$$

where

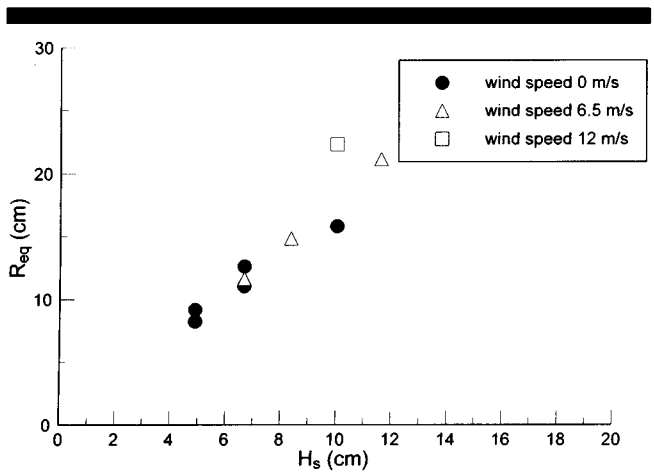


Figure 11. Equivalent runup comparison for 1-sec mechanical waves on a smooth 1:3 slope.

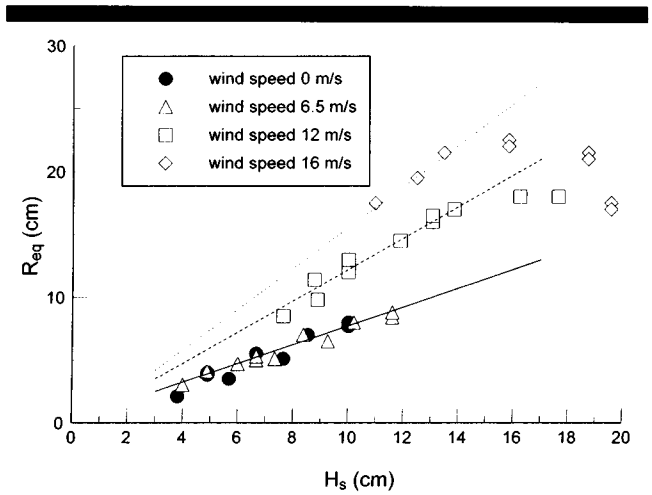


Figure 13. Equivalent runup comparison for 1-sec mechanical waves on a rough 1:1.5 slope.

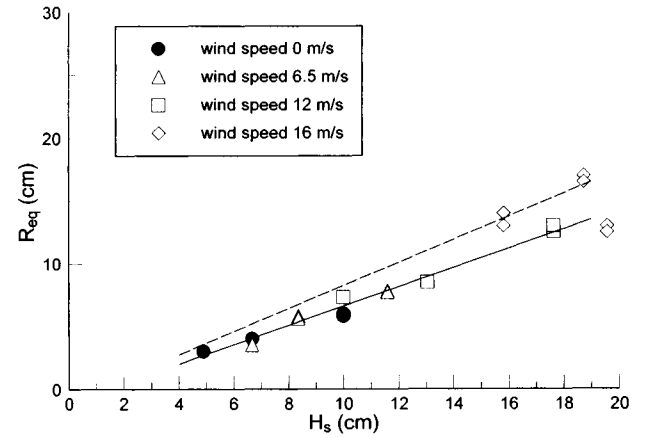


Figure 14. Equivalent runup comparison for 1-sec mechanical waves on a rough 1:3 slope.

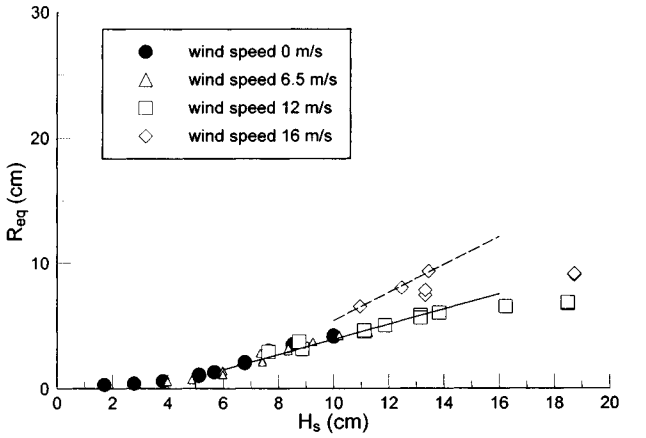


Figure 15. Equivalent runup comparison for 1-sec mechanical waves on a rough 1:5 slope.

$H_{m0}$ = zeroth-moment wave height

$m_0$ = zeroth moment of the energy spectrum

However, comparing runup to incident wave height is now complicated due to effects of the different wave periods involved. An empirical method of combining both peaks into a single "equivalent" peak was suggested by VAN DER MEER and JANSSEN (1994). An equivalent wave period is weighted by the fourth root of the zeroth moments of each peak as illustrated in Figure 18 and defined by:

$$T_{p(eq)} = \sqrt[4]{\frac{m_0(1)}{m_0}T_p^4(1) + \frac{m_0(2)}{m_0}T_p^4(2)} \quad (2)$$

where

$T_{p(eq)}$ = equivalent peak period for a double-peaked spectrum

$m_0(1)$ = zeroth moment (area) of the peak pertaining to the longer wave

$m_0(2)$ = zeroth moment (area) of the peak pertaining to the shorter wave

$m_0$ = zeroth moment of the spectrum, $m_0(1) + m_0(2)$

$T_p(1)$ = peak period pertaining to the longer wave

$T_p(2)$ = peak period pertaining to the shorter wave

By weighting peak periods with the fourth power of the wave peak period, the longer wave period is much more heavily weighted than the shorter wave. This is intuitively reasonable as longer waves have a much greater effect on runup than shorter waves. Equation 2 then gives us a simple means of reducing a dual-peaked spectrum to an equivalent single peak for comparing effects of wind energy on runup.

It is also common practice to relate runup to a function of the surf parameter or Iribarren number (BATTJES, 1974; WALTON and AHRENS, 1989; AHRENS and HEIMBAUGH, 1988; DE WAAL and VAN DER MEER, 1992; VAN DER MEER and JANSSEN, 1994), defined as structure slope over square root of wave steepness:

$$\xi = \frac{\tan\theta}{\sqrt{\frac{H}{L_0}}} \quad (3)$$

where

$\xi$ = surf parameter

$\theta$ = structure slope with the horizontal

$H$ = incident wave height

$L_0$ = deepwater wavelength

The surf parameter is convenient for combining structure slope, wave height, and wave period (or wave length) into a single parameter. Its effectiveness in defining runup is due to its relationship to the breaking wave environment, where a smaller surf parameter implies a more severe breaking wave climate.

Using the equivalent peak wave period, $T_{p(eq)}$, defined in

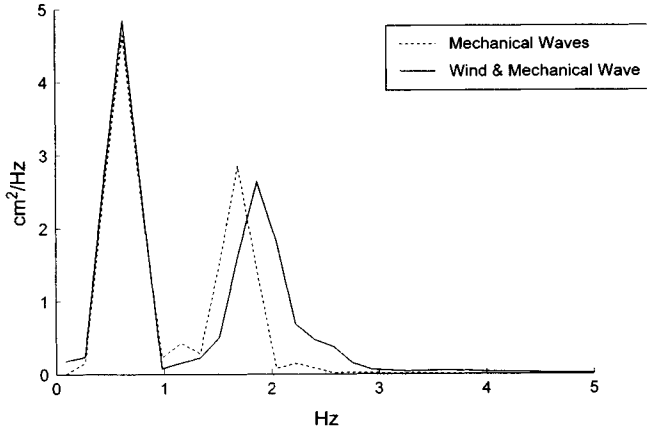


Figure 16. Comparison of energy spectra for wind/wave spectrum and mechanically-reproduced wind/wave spectrum.

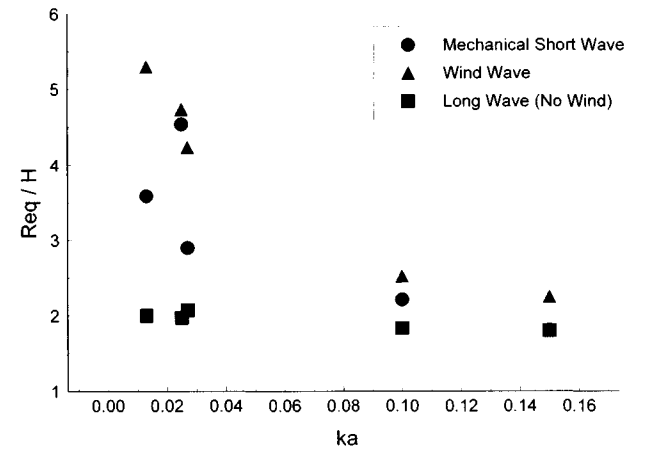


Figure 17. Runup comparison for wind/wave spectrum and mechanically-reproduced spectrum on 1:3 smooth slope.

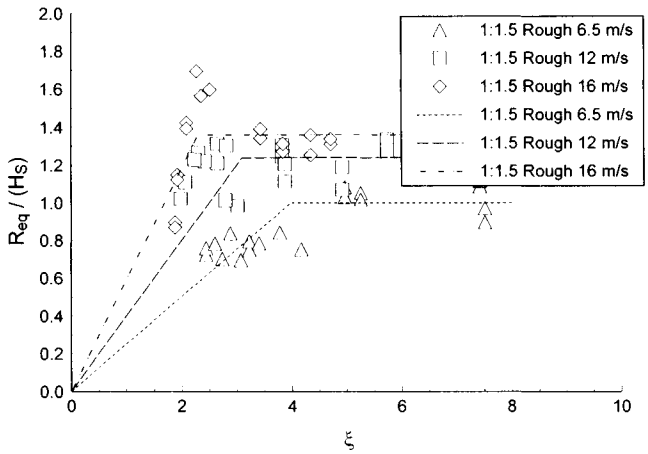


Figure 19. Wave runup predictions including wind effects for a 1:1.5 rough slope.

Equation 2 to calculate deepwater wavelength, and wave height determined from the zeroth moment of the entire spectrum by Equation 1, a surf parameter may be determined for dual-peaked spectra. Figures 19 through 21 plot relative runup versus surf parameter for the 1:1.5, 1:3, and 1:5 rough slopes, respectively. Although the surf parameter includes structure slope, the data is separated by slope in Figures 19 through 21 to simplify the plots and more clearly illustrate trends in the data.

Equations presented in VAN DER MEER and JANSSEN (1994) show relative runup increasing linearly with the surf parameter up to a maximum value. Beyond this maximum value, relative runup remains constant for increasing values of the surf parameter. Similar trend lines have been fitted to the data in Figures 19 through 21 to more clearly illustrate the wind effects.

Figures 19 through 21 show the effects of wind on runup are greater for steep slopes, with runup on the 1:1.5 slope revetment being about 40 percent greater under the influence of the 16 m/sec wind.

## CONCLUSIONS

Tests conducted in a wind/wave flume have demonstrated that runup elevations in a physical model study may be considerably greater if the study is conducted under the influence of strong onshore winds. After separating out effects of wind-induced setup and wind-induced wave growth, significant increases in runup elevations were observed during tests conducted under the influence of wind. Increases in runup due to wind effects were greatest on steeply-sloped structures (1:1.5), with only minor increases under strong winds observed for flat slopes (1:5). Increases in runup were observed both on smooth slopes and rough slopes, with greater increases observed on the smooth slopes. Stronger winds caused

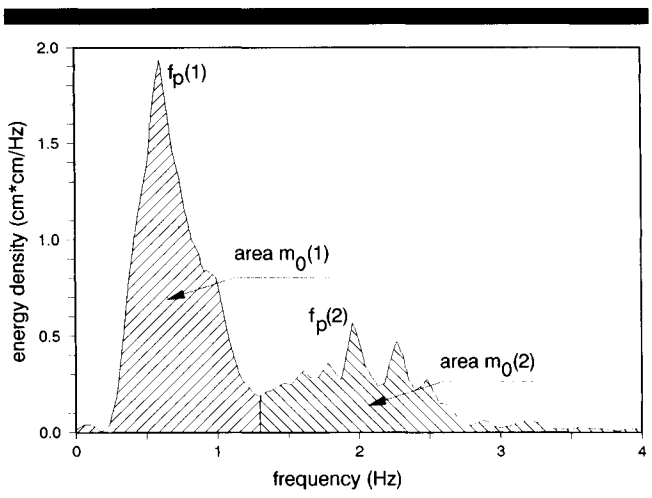


Figure 18. Example of the division of a double-peaked energy spectrum.

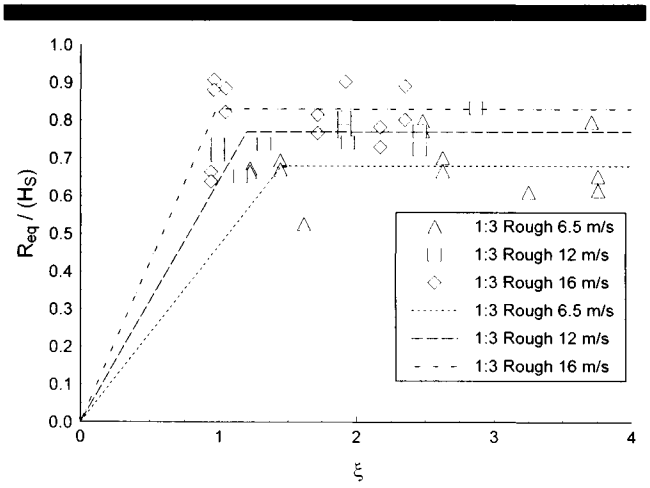


Figure 20. Wave runup predictions including wind effects for a 1:3 rough slope.

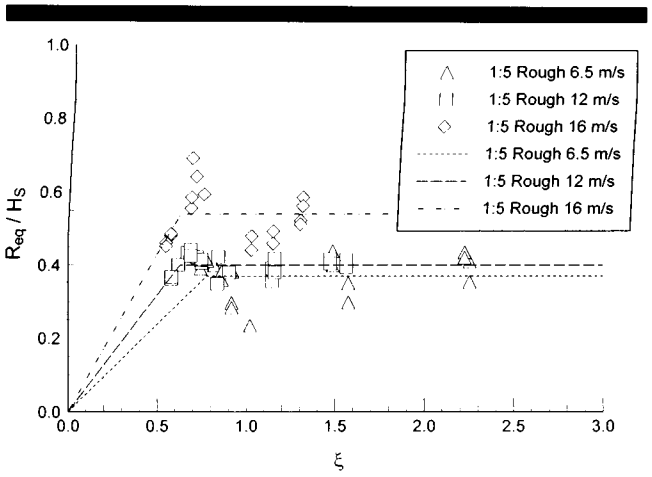


Figure 21. Wave runup predictions including wind effects for a 1:5 rough slope.

greater runup than mild winds, with almost no changes in runup observed at the slowest wind speed tested (6.5 m/sec).

The addition of wind to mechanically-generated wave periods of 1.75-sec or longer introduced a second peak into the wave-energy spectra. Dual-peaked spectra are commonly found in coastal areas, and two methods were presented for studying wind effects with dual-peaked spectra. Results again indicated that wind effects may cause significant increases in wave runup elevation.

The significant increases in runup elevations under the influence of wind observed in this study may be attributed to wind effects on the runup bore and/or changes in wave kinematics due to wind effects altering wave shape or affects on wave breaking. Similar to wind-induced wave growth, it is suggested that wind effects on a runup bore include both shear forces and a pressure differential between the shoreward and offshore sides of the runup bore. Wind effects on wave shape that may influence runup include changes in wave steepness or crest/trough characteristics, formation of small wind-induced waves riding on the longer mechanically-produced waves, or an increase in the irregularity of the waves that was not observed due to the resolution of the energy spectra. Wind may also affect runup elevations by imparting an additional horizontal forcing function on the wave at wave breaking.

Although this study has quantified wind effects on runup in a wind/wave flume, the effects of onshore winds on prototype structures is still being investigated. While it is clear that the higher wind velocities used in this study are unrealistic based on typical model scales and Froude model scaling, scaling laws for applying model wind/waves results to the prototype have not been determined as both gravitational effects (Froude scaling) and viscous effects (Reynold's scaling) play an active role. Derivation of appropriate scaling relationships is currently being investigated. Spectral wave conditions, wave groups, and wind/wave directionality also will affect the influence of wind on runup on coastal structures.

## ACKNOWLEDGEMENTS

The writers wish to acknowledge the Office, Chief of Engineers, U.S. Army Corps of Engineers, for authorizing publication of this paper. It was prepared as part of the Design of Revetments and Seawalls work unit in the Coastal Program of the Civil Works Research and Development Program.

## LITERATURE CITED

AHRENS, J.P. and HEIMBAUGH, M.S., 1988. Approximate upper limit of irregular wave runup on riprap. *Technical Report CERC-88-5,* U.S. Army Engineer Waterways Experiment Station, Vicksburg, Mississippi.

AHRENS, J.P. and MARTIN, F.T., 1985. Wave run-up formulas for smooth slopes. Journal Waterway, Port, Coastal and Oceanographic Engineering (ASCE), 111(1), 128–133.

BATTJES, J.A., 1974. Surf similarity. *Proceedings 14th Coastal Engineering Conference,* (Copenhagen, Denmark, ASCE) pp. 465–480.

DE WAAL, J.P. and VAN DER MEER, J.W., 1992. Wave runup and overtopping on coastal structures. *Proceedings 23rd Coastal Engineering Conference,* (Venice, Italy, ASCE), pp. 1758–1771.

GODA, Y. and SUZUKI, T., 1976. Estimation of incident and reflected waves in random wave experiments. *Proceedings 15th Coastal Engineering Conference,* (Honolulu, Hawaii, ASCE), pp. 828–845.

KOBAYASHI, N. and POFF, M.T., 1994. Numerical model RBREAK2 for random waves on impermeable coastal structures and beaches. *Research Report No. CACR-94-12,* Center for Applied Coastal Research, University of Delaware, Newark, Delaware.

KOBAYASHI, N. and WURJANTO, A. 1989. Numerical model for design of impermeable coastal structures, *Research Report No. CE-89-75,* Center for Applied Coastal Research, University of Delaware, Newark, Delaware.

PHILLIPS, O.M. 1984. The dispersion of short wavelets in the presence of a dominant long wave, *Journal Fluid Mechanics,* 107, 465–485.

SHYU, J.H. and PHILLIPS, O.M. 1990. The blockage of gravity and capillary waves by longer waves and currents. *Journal Fluid Mechanics,* 217:115–141.

SOBEY, R.J. 1986. Wind-wave prediction. *Annual Reviews Fluid Mechanics,* 18, 149–172.

U.S. ARMY ENGINEER COASTAL ENGINEERING RESEARCH CENTER. 1995. *Design of Coastal Revetments, Seawalls, and Bulkheads.* Engineering Manual 1110-2-1614, U.S. Government Printing Office, Washington, D.C.

VAN DER MEER, J.W. and JANSSEN, J.P.F.M. 1994. Wave Run-Up and Wave Overtopping at Dikes and Revetments. Delft, The Netherlands: Delft Hydraulics, Publication No. 454.

VAN DER MEER, J.W.; PETIT, H.A.H.; VAN DEN BOSCH; P., KLOPMAN, G., and BROEKENS, R.D., 1992. Numerical simulation of wave motion on and in coastal structures. *Proceedings 23rd Coastal Engineering Conference,* (Venice, Italy, ASCE), 1772–1784.

WARD, D.L., 1992. Prediction of overtopping rates for irregular waves on riprap revetments. Miscellaneous Paper CERC-92-4, U.S. Army Engineer Waterways Experiment Station, Vicksburg, Mississippi.

WARD, D.L.; WIBNER, C.G.; ZHANG, J., and EDGE, B., 1994. Wind effects on runup and overtopping. *Proc. 24th Coastal Engineering Conference,* Kobe, Japan, ASCE, 1687–1699.

WEGGEL, J.R., 1976. Wave overtopping equation. *Proceedings 15th Coastal Engineering Conference,* (Honolulu, Hawaii, ASCE), 3, 2737–2755.

WURJANTO, A. and KOBAYASHI, N., 1991. Numerical model for random waves on impermeable coastal structures and beaches. *Research Report No. CACR-91-05,* Center for Applied Coastal Research, University of Delaware, Newark, Delaware.

YAMAMOTO, Y. and HORIKAWA, K., 1992. New methods to evaluate runup height and wave overtopping rate. *Proceedings 23rd Coastal Engineering Conference,* Venice, Italy, ASCE.

ZHANG, X., 1995. Capillary-gravity and capillary waves generated in a wind wave tank: observations and theories. *Journal Fluid. Mech.,* 289, 51–82.